

Investigating the Effect of Stearic Acid on the Mechanical, Rheological, and Microstructural Properties of AISI 4605 Feedstock for Metal Injection Molding Process

Vahid Momeni¹ · Ali Askari² · Mohammad Hossein Allaei³ · Hadi Zangi⁴

Received: 27 February 2021 / Accepted: 29 April 2021 / Published online: 10 June 2021
© The Indian Institute of Metals - IIM 2021

Abstract Nowadays, the metal injection molding (MIM) process is a manufacturing method to produce complex shape components. Feedstock preparation in this process is vital because produced feedstock defects can be detrimental in the following processing steps. In this study, effect of the percentage of stearic acid (SA) is investigated on the density, strength, hardness, rheological properties, and microstructure of a part made by 4605 low-alloy steel powder using the MIM process. For this reason, feedstock with different percentages of SA from 1 to 17% has been produced. Mechanical and physical properties show that SA, as a surfactant, has two impacts on the results. SA from 1 to 9% improves the powder particle's distribution in the binder system and increases the strength and density of the sintered bodies. The results also indicate that with more surfactant growth, the density and strength dramatically decrease due to lower carbon in the sintered parts. The carbon content determines the final sample's microstructure, which has a substantial influence on the properties. Besides, it can be inferred from the results that the hardness lessens with a gentle slope as the amount of

SA in the binder system increases. From the perspective of rheological properties, more SA results in higher sensitivity of feedstocks to the shear rate.

Keywords Metal injection molding · Stearic acid · Mechanical properties · Surfactant · Density

1 Introduction

Metal injection molding (MIM) is a precise manufacturing process used to produce small to medium components with high complexity in the shape [1, 2]. This process utilizes fine metallic powders (typically less than 20 μm) as raw material, formulated with a binder system (various thermoplastics, waxes, and other materials) into a feedstock. The binder system's composition has received much attention during the recent years [3–12] mainly since the binder system depends on the size, shape, and material of the powder used, and an ideal binder system suitable for all powder systems is still impossible to attain. A successful binder system consists of backbone polymer, filler (most of the time waxes), and surfactant (plasticizer, dispersant, lubricant) [13], although sometimes a binder system component can play multiple roles simultaneously.

Dispersants are used to improve the dispersion of the powder particles and increasing solids loading. Lubricant, a low-molecular-weight polymer, is added to the backbone polymer to decrease the friction between the powder particles and, as a result, decrease the viscosity [14]. The surfactant is added as an additive in the binder system to improve some properties such as spreading, binder strengthening, adsorption, and surface wetting [15].

Generally, the surfactant is a low-molecular-weight component that can adhere to the powder particle's surface

✉ Ali Askari
Ali.Askari@Kiau.ac.ir

¹ Department of Mechanical Engineering, Faculty of Materials and Manufacturing Processes, Malek Ashtar University of Technology, Tehran, Iran

² Department of Mechanical Engineering, NazarAbad Center, Karaj Branch, Islamic Azad University, Karaj, Iran

³ Center for Composite Materials, Faculty of Materials and Manufacturing Processes, Malek Ashtar University of Technology, Tehran, Iran

⁴ Department of Materials Engineering, Faculty of Materials and Manufacturing Processes, Malek Ashtar University of Technology, Tehran, Iran

and improve the connection between the powder particles and binder system components. Therefore, the surfactant acts as a bridge between the binder system and the powder particle due to its particular structure, and it enhances the powder's stabilization when mechanical shearing during the mixing process breaks them away from each other [16]. A surfactant can act as a lubricant, effectively enhancing the adhesion strength between the binder system and the powder particles, improving the strength of green parts and offering a potential way to eliminate structural defects. It can be concluded that surfactant influences the final product's quality and is crucially important to the MIM process [17–24]. Stearic acid (SA) works as a surfactant and acts as a lubricant that enhances the dispersion of powder particles in the binder system during mixing and improves the solids loading and green body strength without sacrificing the mixture's flow properties [25–27].

Yi-min et al. [13] studied the effects of surfactant on the properties of MIM feedstock prepared by 17-4PH stainless steel powder and paraffin wax-based binder containing different contents of the SA as the surfactant. The results showed that the addition of the SA significantly decreases the viscosity of the feedstock. It also decreases the binder's wetting angle with the powder particle, and the critical solids loading increases. The lowest amount of surfactant is calculated to be 0.19%. The experiments indicate that about 5% of the SA is the optimal value to improve the feedstock's mechanical properties. In the powder injection molding (PIM) process, SA can serve as a plasticizer for polymers, as a lubricant between powder particles and machine die walls and as a surfactant between powder particles and binder system. Paul Lin and German [28] claimed that a bulk mixture of powder particles and binder system is challenging to obtain without SA in the binder system. Adhesion of the SA to the powder surface significantly reduces the binder/powder interfacial energy and contact angle but is important when the particle surface area increases.

Suetsugu and White [29] studied the behavior of dispersion of calcium carbonate particles in the palm stearin (PS) matrix. Their results showed that coating the particles with SA dramatically reduces the viscosity and aggregation of particles. Therefore, coating the particles with SA reduces interactions between the particles.

Istikamah Subuki et al. [30] showed that SA's addition significantly reduces the mixing torque value during the mixing and viscosity of feedstock, which corresponds to a decrease in inter-particle friction. As a result, injection molding could be carried out at a lower temperature, and the removal rate of the binder system increases during the solvent extraction process.

According to the aforementioned points and researches about the role and importance of the Stearic Acid and its

role in the MIM feedstocks, in this study, the influences of SA as a part of 4605 low-alloy steel feedstock on the mechanical, rheological, and microstructural properties of the final part have been investigated. Feedstock samples containing different SA percentages are produced and examined for mechanical, rheological, and microstructural properties.

2 Experimental Procedure

Metallic powder and a binder system have been used as the primary materials for manufacturing samples. The powder used in this study includes 4605 low-alloy steel with a powder particle size between 4 and 20 μm , which is the suggested particle size range for MIM powder [31–33]. The powder is from Unifine Company, China, which is manufactured by gas atomization technique. Fig. 1 shows the SEM micrograph of the powder taken by TESCAN, VEGA3. As can be observed, the powders are in a spherical shape, which effectively increases the density, microstructure, and moldability.

The density of the powder is measured by AccuPycTM 1330 Pycnometer, which is 7.95 g/cm^3 . The average particle size of the powder used is an important factor during the sintering process [4], and in this study, it has been measured by Malvern (Mastersizer 2000 model). The particle size distribution of the powder has a high range, as can be observed in Fig. 2. It leads to a less amount of binder system during the process and a higher density of the final part.

To determine the width of the particle size distribution (S_w) for this powder with the values of $33.65 \mu\text{m}$ and $2.55 \mu\text{m}$ for D_{90} and D_{10} , respectively, equation (1) is used [17]

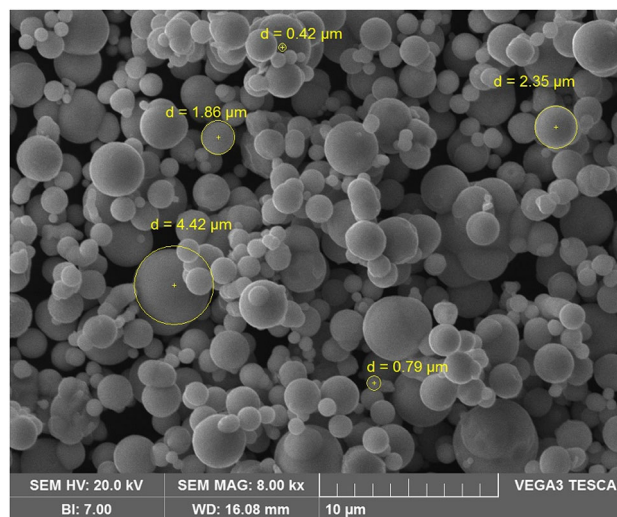
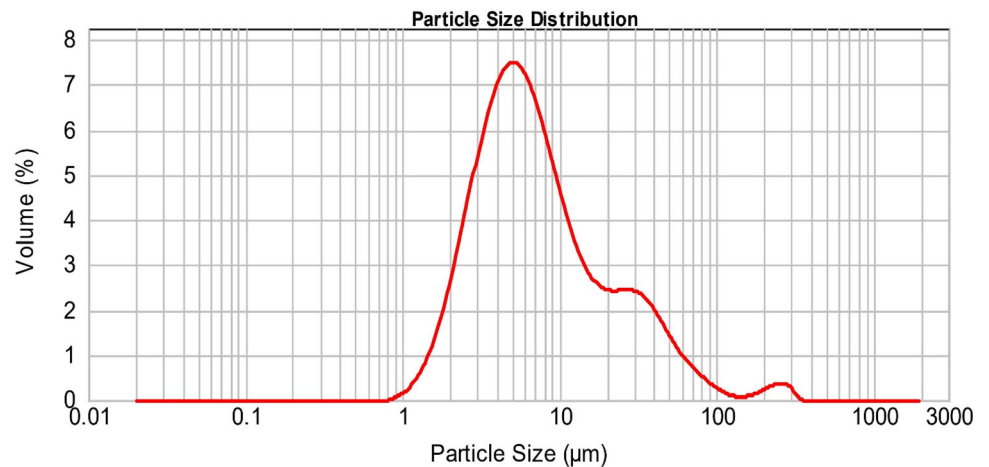


Fig. 1. SEM of 4605 low-alloy steel gas atomized powder

Fig. 2. The particle size distribution of 4605 low-alloy steel powder



$$S_w = \frac{2.56}{\log(D_{90}/D_{10})} \tag{1}$$

For MIM purposes, S_w should be between 2 and 7. A higher value of S_w results in the low size distribution of particles and difficulty during the injection process. A lower value of S_w reduces the density of the final part. The S_w for powder used with the amount of 2.28 make this powder a suitable choice for MIM.

Paraffin Wax (PW) as the primary component, PolyPropylene (PP) as the backbone, Carnauba Wax (CW) as lubricant and controller of viscosity, and Stearic Acid (SA) as surfactant and lubricant are constituents of the binder system used in this study.

In order to have the optimum percentages of SA from a mechanical and rheological point of view, a suitable binder system consisting of 69% Paraffin Wax, 20% PolyPropylene, 10% Carnauba Wax, and 1% SA is chosen. Because this binder system has shown the ideal and standard characteristics for metallic powders, and the interaction between constituents does not produce improper results [25, 34, 35]. With the variation in the SA percentage, new binder systems have been formulated in the next step, all shown in Table 1.

For the feedstock preparation, 66 vol.% of 4605 low-alloy steel powder was mixed with the binder system

Table 1 Binder system constituents and their percentages

Feedstock	PW (Vol.%)	PP (Vol.%)	CW (Vol.%)	SA (Vol.%)
FS1	69	20	10	1
FS2	66.20	19.2	9.6	5
FS3	63.4	18.4	9.2	9
FS4	60.6	17.6	8.8	13
FS5	57.8	16.8	8.4	17

shown in Table 1. Haake rheocord 90 torque rheometer was used to mix the binder system constituents. Mixing was done at temperature of 170 °C and blade RPM of 65 for 30 min for all of the samples. At the beginning of mixing, the mixing blades show high resistance to the rotation, the same as in the study of Pogodina et al. [36], and then it starts to decrease and becomes stable. This minimum stable torque shows the feedstock’s uniformity which is 5, 4, 3.5, 2, and 0.5 Nm for FS1 to FS5, respectively.

After the mixing process, the feedstock was removed as the bulk from the mixer and granulated to be used as a raw material in the injection molding machine. The injection was conducted by the Battenfeld BA230E injection molding machine with an injection pressure of 130 bar and injection temperature of 165 °C. The mold cavity is a tensile testing specimen of MPIF standard 50. Figure 3 shows the three injected green parts of FS1 feedstock.

In this study, debinding was done in two steps. In the first step, some portion of PW and SA was removed using solvent debinding. It was performed by placing the samples in the n-heptane solution at the temperature of 70 °C for 5 hours [25]. The second step of debinding (thermal debinding) was followed by using the study of Momeni et al. [25]. The differential scanning calorimetry (DSC) of the powder was done using NETZSCH, STA 449 F3 Jupiter apparatus to achieve the suitable sintering cycle (Fig. 4). The sintering was done under the argon atmosphere with a heating rate of 10 °C/min upto 1200 °C.

The DSC-TGA apparatus (NETZSCH, STA 449 F3 Jupiter DSC/TGA) was used to determine the melting temperature of binder system components and binder system decomposition, which helped in designing a suitable cycle for debinding step. The testing condition was heating from room temperature to 600 °C with a heating rate of 5 °C/min, in the argon atmosphere. For measuring the density of the sintered samples, the Sartorius CP224S Analytical Balance apparatus was used with the



Fig. 3. Injected green parts of the FS1 sample

Archimedes method and MPIF 42 standard. Tensile testing was performed to determine the strength and elongation of the manufactured samples. For that, Zwick Z50 testing machine (German-made) was used under displacement control of 0.1 mm/min at room temperature and strain rate of 0.0025 min^{-1} , according to the MPIF 50 standard. The Vickers hardness test was also performed with a load of 30 kg (HV30) for 30 seconds.

In the MIM process, it is desired to incorporate a maximum amount of powder with maintaining a sufficient amount of binder system to retain suitable flow behavior. For that, the rheological behavior of the feedstock needs to be investigated. It is being used to quantify the stability of the feedstock during the molding process [10]. The feedstock's rheological behavior was observed using Instron 3211 capillary rheometer under the condition, which was similar to the injection ($165 \text{ }^\circ\text{C}$ and L/D of 30).

3 Results and Discussion

3.1 Rheological Behavior

With an increase in shear rate in the metal injection molding process, the viscosity should decrease such that this trend represents pseudo-plastic behavior. This phenomenon can help the injection molding stage to reduce jetting and desired temperature; meanwhile, it assists injected parts to retain the shape. During the injection molding, the shear rate ranging between 100 and 10000 s^{-1} can usually be exerted on the parts. In this scope, feedstock's viscosity should not exceed $1000 \text{ Pa}\cdot\text{s}$ at the molding temperature [17]. As shown in Fig. 5, an increase in shear rate leads to decreasing the feedstock's viscosity, displaying pseudo-plastic behavior. For pseudo-plastic behavior at a particular temperature, the relation between viscosity and shear rate is defined using Equation (2):

$$\eta = K \cdot \dot{\gamma}^{n-1} \quad (2)$$

where η represents the viscosity, n shows the flow behavior index, K is constant, and $\dot{\gamma}$ defines the shear rate [37]. The value of n can interpret the sensitivity of the material to the shear rate. A low value of n indicates the intense variation in viscosity to the shear rate. In order to produce delicate and complex green parts, this feature is detrimental. In addition, a feedstock with an n -value close to 1 represents Newtonian flow behavior, which is not applicable for the metal injection molding process.

Fig. 4. DSC analysis of the powder used

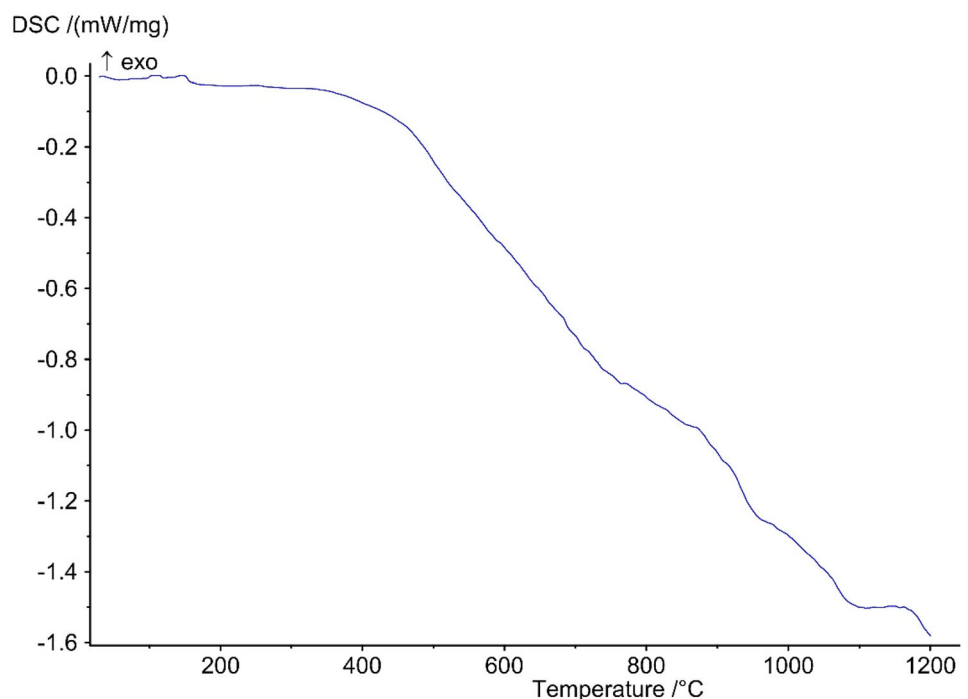
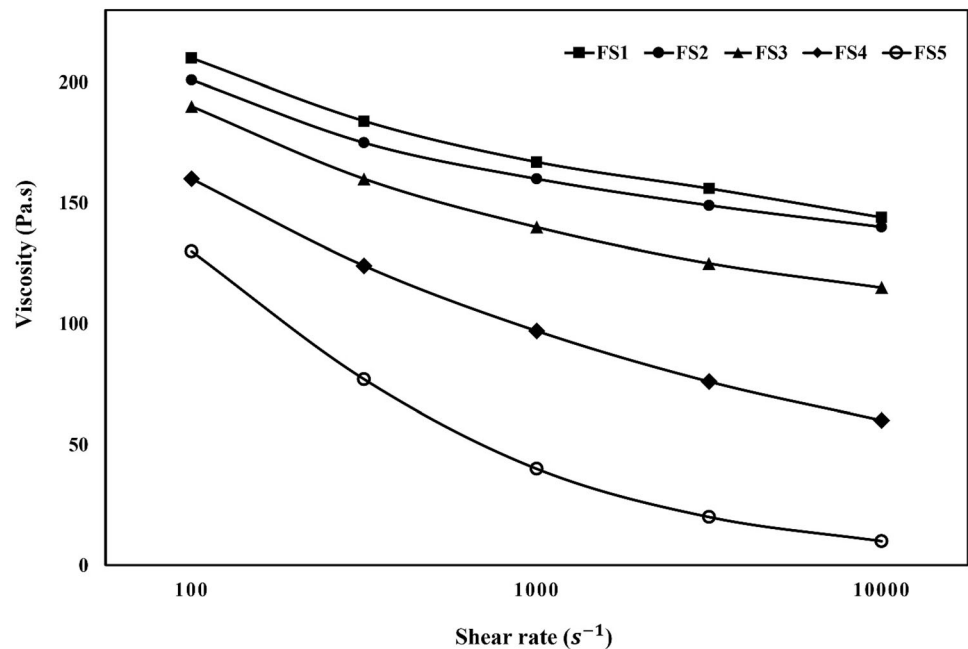


Fig. 5. Viscosity vs. the shear rate for the developed feedstocks



The n -values for all feedstocks are lower than one and are in the order from FS1 to FS5, i.e. 0.92, 0.74, 0.61, 0.47, and 0.29. With the growth in SA percentages, all feedstock's viscosity decreases approximately at the same rate from FS1 to FS3. With more increases in SA from 9 to 17%, the viscosity decreases at higher rates. SA, as a low molecular weight surface active agent, is very efficacious in decreasing the viscosity of feedstock due to its lower intrinsic viscosity and higher polarity [38]. In a lower amount of SA, the powder particles are covered by thin layers of binder constituents, which could reduce the viscosity gradually by increasing SA values from 1 to 9%. However, by accumulating more layers around particles and between them by varying SA from 9 to 17%, the viscosity can be declined at a higher rate because of a dramatic decrease in friction between powder particles.

It can be inferred from the results that the FS5 is more susceptible to the shear rate. Considering the rheological properties resulting in this study, an increase in the surfactant amount leads to lower viscosity and higher sensitivity to shear rate.

3.2 Physical and Mechanical Properties

The relative density of sintered bodies as a function of the SA percentages in the feedstocks is presented in Fig. 6. It can be observed that there is an optimum point for the proper amount of SA for this powder with the powder loading of 66 vol.%. The density of the parts increases with the increase in SA from 1 to 9%. More growth in the amount of SA leads to a decrease in density remarkably. A

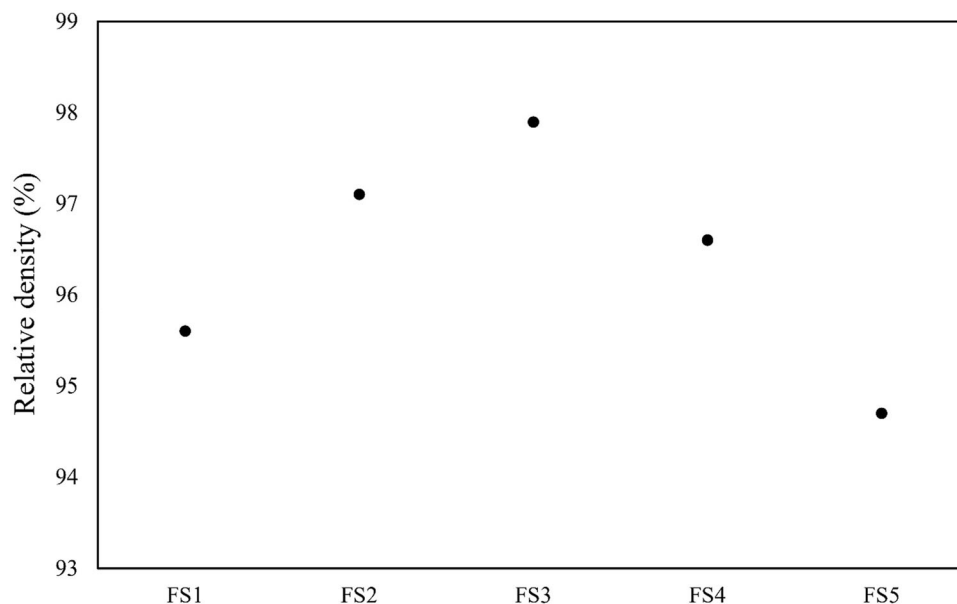
higher amount of SA can improve the physical and mechanical properties by preventing aggregation of powder particles and stabilizing them during high shearing. This is because using SA as a surfactant can provide uniform and sufficient pores after solvent debinding resulting in fewer porosities after sintering. It is possible that for the sample with very high SA values, the pores which are formed in the debinding process are too large that can lead to wide separation between particles during densification by sintering. The result can be non-uniform shrinkage, large porosities, low density, and strength [38].

Spreading of binder constituents on the surface of powder particles is challenging to develop a suitable binder system. For this reason, the surfactant is required to improve the wetting ability for the powder with a decrease in the wetting angle. In this study, an increase in SA has a dual impact. On the one hand, a higher amount of surfactant leads to lessening of diffused carbon from the degradation of PP during the thermal debinding and sintering process. Because from the FS1 to FS5, the amount of PP is reduced, which has the most significant effect on residual carbon [33].

On the other hand, using the proper values of the SA can provide a high-quality dispersion of powder particles in a binder system that can effectively increase density and strength and reduce pores.

Also, the possibility of powder-binder segregation is decreased in this situation. As shown in Fig. 6, a sudden decrease in density from FS3 to FS4 means that the maximum capacity of wettability can be achieved using the 9% SA for this binder system and powder loading of 66 vol.%

Fig. 6. Influence of stearic acid on the relative density of final parts



used in this study. The effects of lower residual carbon on decreasing density and strength represent itself with more growth in SA to 17%. The average values of the mechanical properties of sintered parts are presented in Table 2. The density and strength of the FS5 sample are confronted with a dramatic decrease due to use of 17% surfactant (Fig. 6 and Table 2). The highest relative density and tensile strength measured in the FS3 sample are 97.9% and 546 MPa.

Pores significantly influence the mechanical and physical properties because they can provide stress concentration for samples, leading to failure in the parts. Minimizing the pores should be considered one of the high-priority tasks in determining the final properties during the metal injection molding process. As for density, it almost follows the same trend as strength. The tensile strength grows with SA's increase from 1 to 9%, although the residual carbon decreases in this range. This is explainable by using two reasons. First, improving the wettability from FS1 to FS3 can help the desired arrangement between powder particles before the start of sintering. It can lead to a decrease in size and pores' amount because of lowering distances and places between particles (Fig. 7). Figure 7 shows the dispersion of powder particles in the binder system, assuming

that the SA percentages are not enough for FS1 and FS2. As shown in Fig. 7, the FS1 with 1% SA has large spaces between particles in some areas, and in other regions, the accumulated binder can be seen, which has deleterious effects in the formation of defects in the following steps. Although more SA in FS2 presents a better dispersion of particles than FS1, there is still a lack of uniformity in the feedstock. The FS3 with 9% SA represents the most uniform dispersion for this powder.

It can be concluded that the effect of increasing density outweighs the decreasing carbon on tensile strength from FS1 to FS3. Secondly, some specific impacts of the residual carbon left from the degradation of PP during the debinding and sintering phase could be a factor that creates these changes. More investigation will be done from the microstructure point of view in the following sections. The hardness values have a completely different trend from density and strength. With an increase in the amount of SA, the hardness of sintered parts is reduced by decreasing carbon content. On the contrary, the final parts' elongation decreases in which the FS5 specimen shows the highest elongation and the lowest hardness.

3.3 Microstructural Properties

The values of the total porosity for FS3 and FS5 estimated by MIP software can be observed in Fig. 8. The amount of approximated porosity in FS3 is 0.36%, lower than 3.05% for FS5. The difference between pores percentage in Fig. 6 and estimated results by the software is logical because the estimated values are local and are obtained from images taken. It can be seen that variation in the SA content leads to a significant microstructure change for the samples.

Table 2 Tensile and hardness test results of sintered parts

Feedstock	FS1	FS2	FS3	FS4	FS5
Tensile Strength (MPa)	479	518	546	513	461
Hardness (Hv)	231	226	218	214	209
Elongation (%)	4.1	4.4	4.8	5.1	5.4

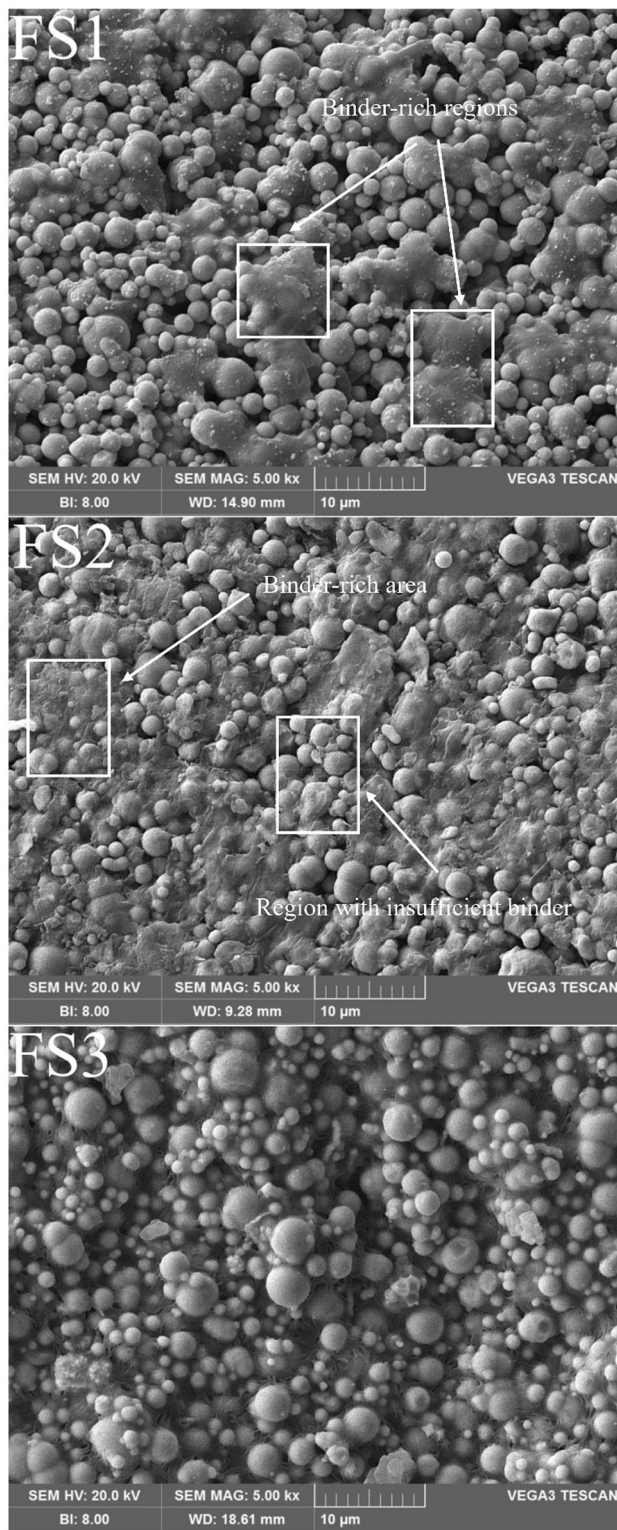


Fig. 7. Distribution of powder particles through the binder system for FS1, FS2, and FS3

While the total porosity of FS3 is low, the FS5 shows a high total porosity, which can be the demonstrator of the lowest density of the sample.

Several steps occur in liquid phase sintering, including powder particles' rearrangement, leveling of particles' melted surface, and filling large pores with grains' growth. Regarding the amount of melted phase, the formation of pores is done in the second step [33]. When the pores have the same size as the particles of powder, pores enter the inside of grains instead of grain boundaries. As a result, the pore-filling process is implemented at a subsided speed because the diffusion rate in the grains is much lower than the diffusion speed in the grain boundaries. The SEM image of the microstructure for FS3 can be seen in Fig. 9. It can be observed that FS3 consists mostly of pearlite, a lower amount of proeutectoid ferrite, and in some cases, the upper bainite phase, which has grown in the form of the Widmanstatten structure. As it has been mentioned that the increase in the amount of SA means lower PP, which is the main reason for residual carbon. For this reason, the possibility of the liquid phase sintering is decreased for FS4 and FS5.

Figure 10 presents the SEM images of the microstructure of FS3 and FS5, which have the highest and lowest density, respectively. The BELEC apparatus for the spectrometry test was employed to measure residual carbon content in all samples. The results show that the FS1 to FS5 have 1%, 0.88%, 0.69%, 0.56%, and 0.51% carbon, respectively. The phase fraction of proeutectoid ferrite compared to pearlite in Fig. 10 verifies the spectrometry test' results that the carbon amount of the FS5 sample is lower than that of the eutectoid point. It can be concluded from the results that the liquid phase sintering may be formed slightly in the FS4 and FS5. In this case, condensation cannot be done significantly, and the results are large pores in the sintered parts. This point can also imply that the pearlite grain size of FS5 is larger than FS3 because the diffusion energy is consumed for surface diffusion instead of condensation. An increase in carbon content results in liquid phase sintering, improving the density of sintered parts.

On the other hand, if the amount of liquid phase is lower than a specific limit, it can be a detrimental factor because the liquid phase is formed only in a limited time. As has been mentioned above, the pores have entered inside the grains because of this phenomenon. The rate of diffusion is low inside the grains and makes the filling of pores a prolonged process. Regarding the spectrometry test, the amount of carbon in the samples of FS1, FS2, and FS3 is higher than this critical limit. In this situation, the high residual carbon has led to less porosity and higher density due to the local melting effect reported in many studies [39, 40]. In these studies, it has been reported that an increase in carbon content increases regions with local melting.

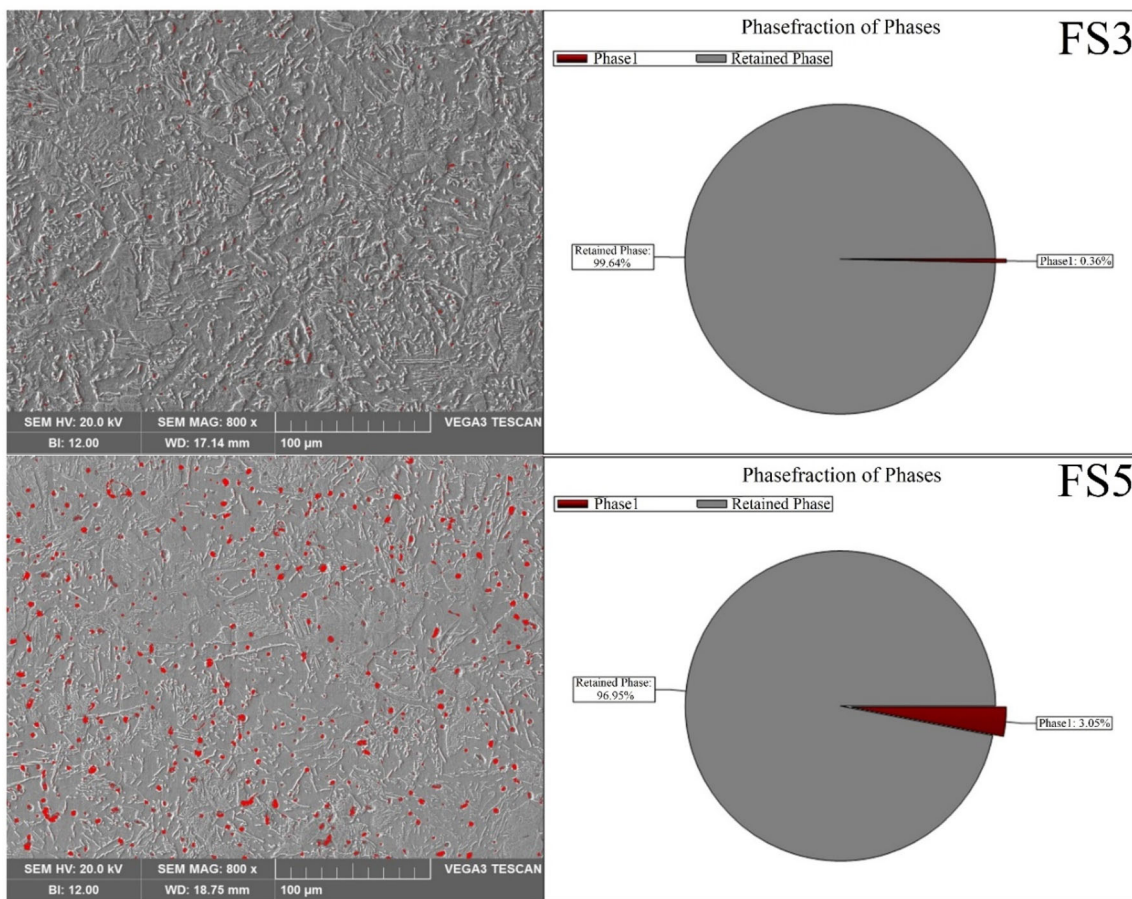


Fig. 8. Estimation of pore percentage for FS3 and FS5 sintered parts, using MIP software

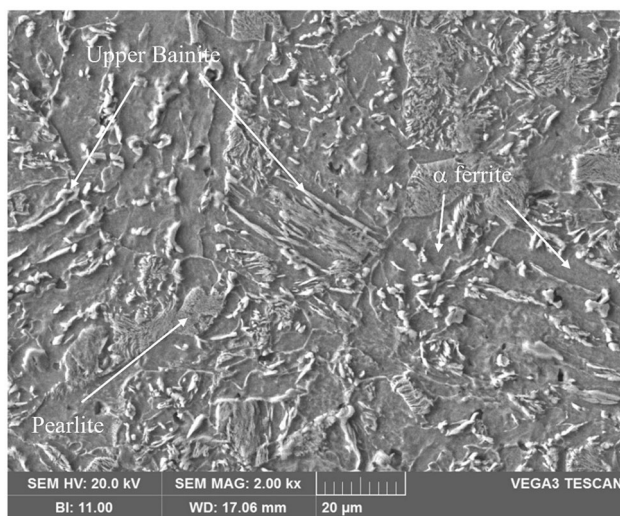


Fig. 9. The phase constituents of the FS3 sample

In this study, it can be concluded that the surface melting of the powder particles is determined by the residual carbon from the burning of binder constituents, especially PP, in the FS1, FS2, and FS3. Also, the iron

melting point is reduced by increasing carbon at the periphery of the powder particles, and under this condition, the grain size is increased dramatically with the growth in carbon content. Although the FS1 sample has higher carbon compared to FS3 and as a result, the melted phase in FS1 (1% C) is higher than FS3 (0.69% C), the density of the FS3 is more than FS1. The reason is that, there are large pores in the FS1 sample because of the low amount of surfactant concerning the high powder loading. This reason results in a poor particle distribution and finally leads to large pores, which this melted phase cannot even fill.

The residual carbon content in the FS5 sample, determined using the spectrometry test, shows a value of 0.51%. In this sample, the microstructure is similar to FS3 (0.69% C). The main difference between the FS3 (0.69% C) microstructure compared to FS5 (0.51% C) is the phases' size. In the FS5 sample, compared with FS3, the lower the amount of pearlite, more proeutectoid ferrite phases have been formed. Also, there is not any trace of a formed upper bainite phase in the FS5. It is clear from Fig. 10 that the carbon content of FS3 is higher than FS5 since the proportion of pearlite to proeutectoid ferrite is increased for the FS3 sample. Because the powder is similar for all

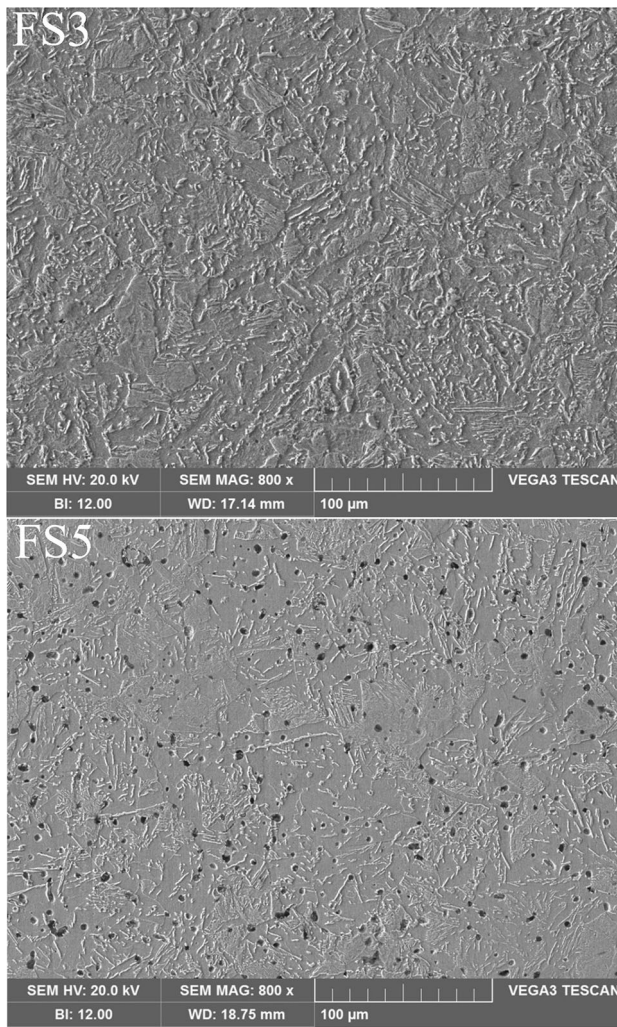


Fig. 10. The microstructure of the FS3 and FS5 samples

sintered parts, it can be inferred that an increase in SA leads to a decrease in PP, resulting in the more residual carbon content of the parts and a significant change in their microstructure. Residual carbon in FS1 measured using the spectrometry test has been found to be 1%. The microstructure of FS1 (1% C) is similar to FS2 (0.88% C). They consist of proeutectoid cementite and pearlite; with this difference, the amount of cementite in the FS2 is lower than FS1. Due to the low cooling rate, a remarkable amount of Widmanstätten cementite phase is formed in the FS1 sample.

4 Conclusion

This study shows that the mechanical, physical, rheological, and microstructural properties of MIM compacts can be affected by using different stearic acid (SA) percentages. From the rheological properties point of view,

feedstock resulting with more SA have shown higher sensitivity to shear rate. Regarding the lower viscosity of the SA comparative to other binder constituents, the overall viscosity of the feedstock has been found to lessen with the increase in SA content. It is confirmed that the density and strength improve to a certain extent with the increase in SA content. The surfactant's proper value is 9%, which has led to the optimum distribution of particles for this powder, binder, and powder loading. After 9% SA as the surfactant, sintered parts' strength and density decrease significantly because of the low carbon amount. However, the hardness decreases slowly with more SA in the feedstock. The elongation is opposite to the hardness trend with a similar slope. It can be concluded that the microstructure of sintered parts plays an essential role in determining of final parts' properties. The variation in type and size of phases in the microstructure is achieved by changing the SA percentage in feedstocks. It is observed that the FS3 sample has similar phases to FS5, but the amount of pearlite to ferrite is higher for FS3, which can be the reason for better properties. As can be inferred from this study's result, the residual carbon left from the binder's burning with different percentages of SA has a remarkable impact on microstructure. The quick and partial formation of liquid phase sintering causes grain growth and produces large voids in the sintered parts. The difference in the diffusion rate inside grains and grain boundaries explains the microstructure change for the sintered parts.

Reference

- [1] Askari A, Alaei M, Nekouee K, Omrani A, and Park S, *Mater Res Express* (2019). <https://doi.org/10.1088/2053-1591/ab4f26>.
- [2] Momeni V, and Alaei M H, *Modares Mech Eng* **19** (2019) 1199.
- [3] Yang B, and German R M, *Tungsten Refract Met* **2** (1994) 237.
- [4] Yang B, and German R M, *Int J Powder Metall* **33** (1997) 55.
- [5] Li Y, Qu X, Li Z, and Huang B, *Trans Nonferrous Met Soc China* **8** (1998) 576.
- [6] Miura H, Morikawa H, Kawakami Y, and Ishibashi A, Development of high performance ferrous sliding abrasive wear resistant materials through power injection molding, in 1998 Int Conf Exhib Powder Metall Part Mater (1999) p 5.
- [7] Kim, S-W, Ryu J-S, and Moon I-H, Ball milling effect on the powder characteristics in metal injection molding of W-Cu powder, in PM 2 TEC 2000 2000 Int Conf Powder Metall Part Mater (2000) p 4.
- [8] Suri P, Atre S V, German R M, and de Souza J P, *Mater Sci Eng A* **356** (2003) 337. [https://doi.org/10.1016/S0921-5093\(03\)00146-1](https://doi.org/10.1016/S0921-5093(03)00146-1).
- [9] Turker M, and Karatas C, *Powder Metall* **47** (2004) 49.
- [10] Fan J, Huang B, and Qu X, *Rare Met Mater Eng* **34** (2005) 367.
- [11] Khakbiz M, Simchi A, and Bagheri R, *Mater Sci Eng A* **407** (2005) 105. <https://doi.org/10.1016/j.msea.2005.06.057>.
- [12] Kim S-W, Suk M-J, and Kim Y-D, *Met Mater Int* **12** (2006) 39. <https://doi.org/10.1007/BF03027521>.

- [13] Li Y M, Liu X Q, Luo F H, and Yue J L, *Trans Nonferrous Met Soc China (English Ed.)* **17** (2007) 1. [https://doi.org/10.1016/S1003-6326\(07\)60039-9](https://doi.org/10.1016/S1003-6326(07)60039-9).
- [14] Yi-min L, Xiang-quan L, Feng-hu L, and Jian-ling W E, *Trans Nonferrous Met Soc China* **17** (2007) 1.
- [15] Tardos G I, Khan M I, and Mort P R, *Powder Technol* **94** (1997) 245. [https://doi.org/10.1016/S0032-5910\(97\)03321-4](https://doi.org/10.1016/S0032-5910(97)03321-4).
- [16] Setasuwon P, Bunchavimonchet A, and Danchaivijit S, *J Mater Process Technol* **196** (2008) 94. <https://doi.org/10.1016/j.jmatprotec.2007.05.009>.
- [17] German RM, and Bose A, *Injection Molding of Metals and Ceramics*, Metal Powder Industries Federation (1997).
- [18] Chan T-Y, and Lin S-T, *J Am Ceram Soc* **78** (1995) 2746. <https://doi.org/10.1111/j.1151-2916.1995.tb08050.x>.
- [19] Martyn M T, James P J, and Haworth B, *Adv Hard Mater Prod* **5** (1988) 10.
- [20] Yan L, Si W, Xiong T, and Miao H, *Rare Met Mater Eng* **33** (2004) 534.
- [21] Romdhane M R B, Baklouti S, Bouaziz J, Chartier T, and Baumard J-F, *J Eur Ceram Soc* **24** (2004) 2723. <https://doi.org/10.1016/j.jeurceramsoc.2003.09.014>.
- [22] Moballeghe L, Morshedian J, and Esfandeh M, *Science* **59** (2005) 2832. <https://doi.org/10.1016/j.matlet.2005.04.027>.
- [23] Wright J K, Edirisinghe M J, Zhang J G, and Evans J R G, *J Am Ceram Soc* **73** (1990) 2653.
- [24] Pugh R J, and Bergstrom L, *Surface and Colloid Chemistry in Advanced Ceramics Processing*, CRC Press, London (1993). <https://doi.org/10.1201/9780203737842>.
- [25] Momeni V, Hossein Alaei M, Askari A, Hossein Rahimi A, and Nekouee K, *Materwiss Werksttech* **50** (2019) 432. <https://doi.org/10.1002/mawe.201800090>.
- [26] Momeni V, Askari A, Alaei M H, Rahimi A H, Nekouee K, and Zangi H, *Trans Indian Inst Met* **72** (2019) 1245. <https://doi.org/10.1007/s12666-019-01615-1>.
- [27] Askari A, Allaei M H, Mehdipoor Omrani A, and Nekouee Kh, *Modares Mech Eng* **19** (2020) 1079.
- [28] Lin S T P, and German R M, *J Mater Sci* **29** (1994) 5367. <https://doi.org/10.1007/BF01171549>.
- [29] Suetsugu Y, and White J L, *J Appl Polym Sci* **28** (1983) 1481. <https://doi.org/10.1002/app.1983.070280421>.
- [30] Subuki I, Ismail M, Amir A, and Omar MA, *J Teknol (Sciences Eng)* **59** (2012) 173. <https://doi.org/10.11113/jt.v59.2587>.
- [31] Gerling R, Aust E, Limberg W, Pffuff M, and Schimansky F P, *Mater Sci Eng A* **423** (2006) 262. <https://doi.org/10.1016/j.msea.2006.02.002>.
- [32] Momeni V, Alaei M H, Askari A, Rahimi A H, and Nekouee K, *Met Sci Heat Treat* **61** (2020) 777. <https://doi.org/10.1007/s11041-020-00499-z>.
- [33] Momeni V, Zangi H, and Allaei M H, *Powder Metall* **63** (2020) 27. <https://doi.org/10.1080/00325899.2019.1701812>.
- [34] Miura H, and Matsuda M, *Process Microstruct Control* **43** (2002) 343.
- [35] Hausnerova B, *Adv Mater Proc* **2** (2017) 761. <https://doi.org/10.5185/amp.2017/873>.
- [36] Pogodina N V, Cerclé, C, Avérous, L, Thomann R, Bouquey M, and Muller R, Processing and characterization of biodegradable polymer nanocomposites: detection of dispersion state, in *Annu Eur Rheol Conf* (2008) pp 543–553. <https://doi.org/10.1007/s00397-007-0243-2>.
- [37] Huang B, Liang S, and Qu X, *J Mater Process Technol* **137** (2003) 132.
- [38] Wen J, Xie Z, Cao W, and Yang X, *J Adv Ceram* **5** (2016) 321. <https://doi.org/10.1007/s40145-016-0205-1>.
- [39] Lal A, and German R M, *Acta Mater* **47** (1999) 4615.
- [40] Li D, Hou H, Liang L, and Lee K, *Int J Adv Manuf Technol* **49** (2010) 105. <https://doi.org/10.1007/s00170-009-2398-8>.

Publisher's Note Springer Nature remains neutral with regard to jurisdictional claims in published maps and institutional affiliations.